VNU Journal of Science: Mathematics - Physics
Journal homepage: https://js.vnu.edu.vn/MaP

Original Article

Influence of Wrinkle Structure on Properties of Na-doped ZnO Films

Bui Nguyen Quoc Trinh[1,*], Pham Nhat Minh[2]

[1]*VNU Vietnam Japan University, Luu Huu Phuoc, Nam Tu Liem, Hanoi, Vietnam*
[2]*University of Science and Technology of Hanoi, 18 Hoang Quoc Viet, Cau Giay, Hanoi, Vietnam*

Received 17 May 2024
Revised 16 June 2024; Accepted 20 June 2024

Abstract: Un-doped ZnO and Na-doped ZnO (NZO) thin films with various Na doping concentrations were successfully fabricated on glass substrates by a sol-gel process. The effect of Na ions at concentrations of 0, 1, 2, 3, 4, and 5% on the crystalline structure, surface morphology, and optoelectronic properties of ZnO films was studied using appropriate measurement techniques. XRD analysis revealed a polycrystalline hexagonal wurtzite structure in the NZO films. The NZO films' average crystal size ranged from 17.7 nm to 19.6 nm. SEM micrographs showed that wrinkle network appeared in the pure and doped ZnO films due to solvent evaporation during the thermal annealing process. UV-Vis spectroscopy pointed out that the average transmittance of NZO films is as large as ca. 78%. The optical bandgap of the films varied slightly between 3.235 eV for the pure ZnO and 3.246 eV for the Na 5% doped NZO film. When Na ions were doped into the NZO films, the electrical conductivity improved. Moreover, the absorption figure of merit exhibited the largest value of 0.981 $\Omega^{-1}cm^{-1}$ for the fabricated NZO films, which enables the use of these films for solar cells and for other optoelectronic applications.

Keywords: Na-doped ZnO, wrinkle network, absorption figure of merit.

1. Introduction

The research and development of applications using n-type materials such as ZnO, In_2O_3, ITO have always attracted attention over the years because of their transparent properties, higher charge transfer efficiency and smaller effective mass for electrons. However, the shortage of p-type semiconductors has made the development of electrical and photovoltaic devices challenging. As a result, finding high-

* Corresponding author.
E-mail address: trinhbnq@vnu.edu.vn

https//doi.org/10.25073/2588-1124/vnumap.4937

performance p-type transparent conductive oxide (TCO) materials will be a major step forward in the development of complex applications.

For semiconductor technology, the search for new pure p-type materials is extensive challenging, so the development of doped semiconductor materials will be an alternative to meet the development of photovoltaic applications. ZnO is one of the potential transparent semiconductor materials in photovoltaic applications because ZnO has a direct wide bandgap of 3.37 eV and a large exciton binding energy of 60 meV at room temperature [1, 2]. ZnO has n-type conductivity due to native defects such as Zn interstitial (Zn_i) and O-vacancy, as well as unintentionally incorporated hydrogen during crystal growth [3]. Furthermore, because ZnO has a flexible host lattice that can accept a wide range of dopant substitutions, the formation of a p-type film of ZnO will result in a multitude of intriguing and ostensibly controllable properties.

Fan et al., [4] showed that achieving p-type ZnO doping is quite difficult due mainly to the self-compensating effect from native defects. Many attempts have been concentrated to generate p-type ZnO using group V elements (N [5], P [6], As [7] and Sb [8]) substituting for O position to the IA group (Li [9], Na [10], K [11]) for Zn position. Theoretically, Lee and Chang [12] demonstrated that group I elements as p-type dopants in ZnO are much better than group V elements. Furthermore, doping is in the cationic position in ZnO semiconductors generally produce a shallower acceptor level than dopants at the anionic site, so the group I elements are likely to act as an acceptor in p-type ZnO [13]. Among group I elements, Na exhibits high stability of acceptors because the bounding energy of Na – O (256 kJ/mol) is much larger than that of Zn – O (159 kJ/mol). Moreover, the formation energy of substituted Na (Na_{Zn}) is much smaller than that of Na_i under O-rich conditions, as studied by Lee and Chang [12]. Park et al., [13] showed that Na can induce shallower acceptor states of 170 meV, making them ideal doping agents for p-type ZnO. In addition, since Na has an electronic shell structure and size that is different from that of Zn, Na element is considered as a good candidate to change the structure, optical, physical and chemical properties of the doped ZnO.

Na-doped ZnO films (NZO) have been fabricated by various methods to explore the effects of Na ions on the properties of ZnO structures. Lin et al., [14] fabricated the NZO films by pulsed laser deposition method to combine with the Al-doped ZnO n-type film for light-emitting diodes application. They indicated that the acceptor level of Na is around 164 meV by temperature-dependent photoluminescence and low-temperature photoluminescence excitation spectra. Ding et al., [15] reported that Na-doped ZnO films synthesized by plasma-assisted molecular beam epitaxi is a p-type film with a hole concentration of 1.81×10^{15} cm^{-3}, Hall mobility of 0.402 cm^2 $V^{-1}s^{-1}$, and resistivity of 8,575 Ωcm, respectively. The sol-gel method is also used to synthesize Na-doped ZnO films according to the study of Wang et al., [16]. Na-doped ZnO thin films with doping contents of 3.0 - 30 at.% exhibited a hexagonal polycrystalline structure. The optical band gap initially increased and then decreased nearly linearly with the increase of Na content. Cuadra et al., [17] studied the influence of Na and K on the electrical properties of ZnO prepared by spray pyrolysis deposition onto a soda-lime glass substrates. The doped film exhibited a single hexagonal phase of the wurtzite structure. The optical energy band gap of doped ZnO films increased from 3.27 to 3.29 eV by doping with Na and K, respectively. The electrical resistivity of the undoped ZnO could be decreased from 1.03×10^{-1} pW.cm to 5.64×10^{-2} W.cm (K-doped) and 3.18×10^{-2} (Na-doped), respectively. Among these techniques, the sol-gel method has several significant advantages, including lower equipment costs, ease of composition control at the molecular level through the use of different precursors as dopant sources, and the ability to use different substrates.

However, to our knowledge, no study on Na-doped ZnO films have been conducted that have calculated the relationship between optical and electrical properties. Because a combination of the electrical and optical properties of the film is proven to effectively evaluate transparent conductive thin

films for photovoltaic devices when compared to solar spectrum. Thus, in this work, NZO films with Na doping contents ranging from 0 to 5% was evaluated for photoelectric property relationships using the absorption figure of merit *(a-FOM)* value. Furthermore, the effect of Na on ZnO nanostructures will be investigated for structure-morphological-electro-optical correlations to achieve high-quality NZO thin films.

2. Experimental Procedures

A 0.5 M homogeneous precursor solution was prepared by zinc acetate dihydrate, $Zn(CH_3COOH)_2.2H_2O$ and sodium acetate trihydrate, $NaCH_3COOH.3H_2O$ as a source of dopant with doping ratios of 1, 2, 3, 4, and 5%. The precursor was dissolved in an absolute ethanol solvent and monoethanolamine MEA as a stabilizing agent with the molar ratio of Zn^{2+} and MEA at 1 : 2. Then, the mixture was stirred at 75 °C for 90 min to allow the hydrolysis reaction to take place completely and get a clear and transparent sol. Prior to depositing, the glass substrates were cleaned with ethanol, acetone and DI water for 5 min in an ultrasonic bath to remove organic contamination. Next, these substrates were treated in HF 1% solution for 30 s to improve hydrophilic ability of the sample surface and then rinsed with DI water. After that, Na-doped ZnO thin films were deposited on the cleaned substrates by spin-coating technique with 1,500 rpm for 40 s. The samples were dried at 90 °C for 3 min each layer to evaporate the solvent and remove organic residuals. Finally, the samples were annealed at 550 °C for 30 min in ambient conditions to obtain crystalline films. The crystal structures of Na-doped ZnO thin films were analyzed by X-ray diffraction (XRD, Bruker) and the scanning range of 2θ was between 10° and 70°. The surface morphology of the as-grown ZnO was observed using Scanning Electron Microscopy (SEM, JEOL JSM-IT100). UV-Vis spectroscopy (Shimadzu UV-2450) was used to analyze the optical transmittance of films in the range of 350-800 nm, meanwhile, the film's electrical property was evaluated using a four-point probe measurement (Jandel Model RM3000).

3. Results and Discussion

3.1. XRD analysis

Fig. 1 shows XRD patterns of Na-doped ZnO thin films deposited on the glass substrates with different Na concentrations. All samples exhibited distinct peaks corresponding to the (100), (002), (101), (102), (110), (103), (112) planes (JCPDS 36-1451). It shows that NZO films exhibited polycrystalline hexagonal wurtzite. In Fig. 1, no peak of the Na element or its oxides was observed in the XRD pattern at different doping levels, this indicates that these samples were single phase and Na^+ might effectively substitutes into Zn^{2+} sites in the ZnO lattice, without affecting the crystal structure of ZnO. When the doping concentrations were 2% and 3%, the peak intensity (101) of the film was the highest and was stronger than that of (002) and (100), indicating that the film had better crystalline quality and [101] orientation was the priority direction for film growth. Kim et al., [18] reported that the improved crystallization quality was due to the presence of Na intercalations near oxygen vacancies, which prevented lattice distortion. Besides, the intensity of the peak (101) gradually decreased as the Na concentration increased. This is because the number of nuclei of ZnO increased as the amount of Na doping increased, resulting in a smaller grain size [19]. Na ions improved the crystallization quality of ZnO films at doping concentrations of 2% and 3%. Furthermore, the results show that the fabrication of Na-doped ZnO films by sol-gel and spin-coating processes tends to result in the growth along (101) direction, while recent reports [16, 20] showed that (002) was the preferred orientation when adding Na

ions. According to the research of Shen et al., [21], doping Na_{Zn} can increase crystal growth in the c-axis direction and Na_i can block this growth, so the Na_{Zn}/Na_i ratio in the NZO thin films may be related to the shift of growth in the preferred direction. This result shows that the growth in the c-axis direction was inhibited and the crystal grain tended to grow along with other directions.

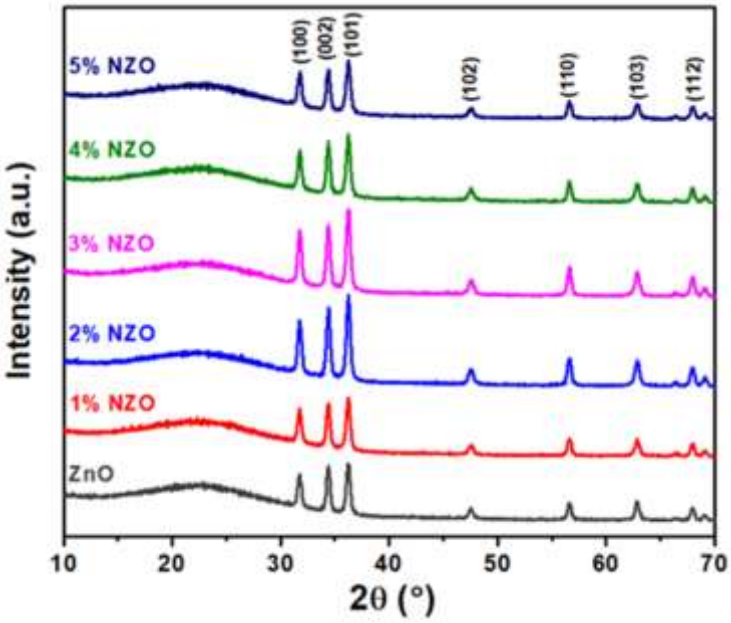

Figure 1. XRD patterns of ZnO thin films with Na doping concentrations varying from 0 to 5%.

Table 1 summarizes FWHM, crystal size *D*, lattice constant *a*, *c*, stress and dislocation density (δ) of (101) peak for all NZO samples.

Average crystal size was calculated by the Scherrer formula [22]:

$$D = \frac{0.9\lambda}{\beta cos\theta} \quad (1)$$

where *D*, λ, β and θ are the average crystal size, the X-ray wavelength (λ = 1.5406 Å), FWHM and Bragg diffraction angle, respectively. As listed in Table 1, the average crystal size of (101) orientation for pure ZnO was 18.4 nm and increased to 19.0 nm for 1% Na doping. Because of the difference in charge and ionic radius between Zn and Na ions, Na ions can occupy both lattice and interstitial positions, increasing in crystal size [23]. The increasing number of nuclei at higher doping concentration may inhibit crystal development, for particular, the size reduces to 17.7 nm when Na concentration is 5%. This trend was also observed in some other studies on Na-doped ZnO and K-doped ZnO [19, 24].

The lattice constants *a*, *c* were calculated using the following formula [25]:

$$\frac{1}{d_{hkl}^2} = \frac{4}{3}\left[\frac{h^2 + hk + k^2}{a^2}\right] + \frac{l^2}{c^2} \quad (2)$$

where *a* and *c* are the lattice constants and d_{hkl} is the crystalline plane distance for indices (*hkl*). The results from Eq. 2 show that the lattice constants *a* and *c* of all the samples show little variation, a = 3.24 Å and c = 5.19 Å. In addition, the lattice constant *a* and *c* are well-matched with data from the standard pattern (JCPDS 36-1451). This proves that a small amount of Na ions did not affect the crystal structure parameters of Na-doped ZnO.

The lattice strain (ε) and dislocation density (δ) of the Na-doped ZnO thin films were estimated by using the following equations [26]:

$$\varepsilon = \frac{\beta}{4\tan\theta} \tag{3}$$

$$\delta = \frac{1}{D^2} \tag{4}$$

The dislocation density can be defined as the length of the deflection lines per unit crystal volume. The dislocation density of the NZO thin film changed as the Na doping concentration increased from 0 to 5%, whereas the lattice strain (ε) did not change significantly in different samples. It means that there was additional new stress in the ZnO background lattice due to the differences in ionic radii of Zn^{2+} (0.74 Å) and Na^{+} (0.95 Å).

Table 1. The FWHM, crystalline size (D), lattice parameters (a, c), strain (ε), dislocation density (δ) values calculated for (hkl) = (101) and 2θ = 36.34°.

Na Doping levels (%)	FWHM (°)	D (nm)	a (Å)	c (Å)	ε	δ (10^{-3} nm)
0	0.449	18.38	3.24	5.19	5.25	1.75
1	0.439	19.04	3.24	5.19	5.25	1.67
2	0.437	19.59	3.24	5.19	5.25	1.67
3	0.469	18.28	3.24	5.19	5.25	1.93
4	0.451	19.20	3.24	5.19	5.25	1.78
5	0.477	17.69	3.24	5.19	5.25	1.99

3.2. Morphological Property

The surface morphology of pure ZnO and NZO thin films was shown in Fig. 2. The un-doped ZnO films has a wrinkle network or ripple structure with skeletal branches, which is considered to be the characteristic structure of ZnO films when other studies also show the same structure [27, 28]. The wrinkled structure was formed by stress relaxation, i.e. the solvent in the film evaporated during drying and induced compressive stress between the film and the substrate, as reported by Kwon et al., [29]. The formation of the wrinkling feature mechanism of sol-gel-derived thin films is different from structurally similar films fabricated by other methods. They demonstrated that the skeleton branches have a satisfying thickness-dependent, $\lambda \sim t_m^{3/4}$ and that the number of skeletal branches depends on the annealing time due to the change in volume strain of the gel film. In addition to the effect of evaporation, the wrinkle formation can be affected by the concentration of Zn^{2+} in the precursor solution [30, 31], and the loss of the hydroxyl/alkoxy group during heating cause conductive stress [32]. In Fig. 2, the pure ZnO film shows a wrinkled network consisting of nanoparticles bound together forming a ZnO porous surface. This is perhaps because the large grain size changes the grain boundaries and leads to the appearance of large defects. When adding Na ions, the wrinkle structure remains the same and the nanoparticles become smaller and more tightly arranged. In the studies, this phenomenon has not been observed when doping Na into the ZnO structure. This indicates that Na ions not only do not change the original structure of ZnO but also help the ZnO film to have a more uniform, denser surface.

The roughness of the ZnO film and the 3% Na-doped film were analyzed by ImageJ software, as shown in Fig. 3. From the data analysis, the film roughness was of 74.60, 70.73, 58.62, 56.74, 56.64 and

60.31 nm with the increase of the Na concentration. It can be seen that the un-doped ZnO film has the highest roughness value compared to the other samples. The roughness of these films formed relatively deep grooves between the veins. With this special structure, the transparent ZnO-based film has better light absorption than other transparent thin films. This leads to a longer path of photons and longer storage in the film and subsequent development into materials in photovoltaic devices. Sekine et al., [33] reported that solar cells with nano-ridge ZnO films improved by about 25% compared with similar devices made with flat ZnO films. In addition, Choi et al., [34] tested the Organic Tandem Solar Cells device and showed that using ZnO's nano-ripple patterned device also improves the power conversion efficiency by about 30% compared to the unpatterned device.

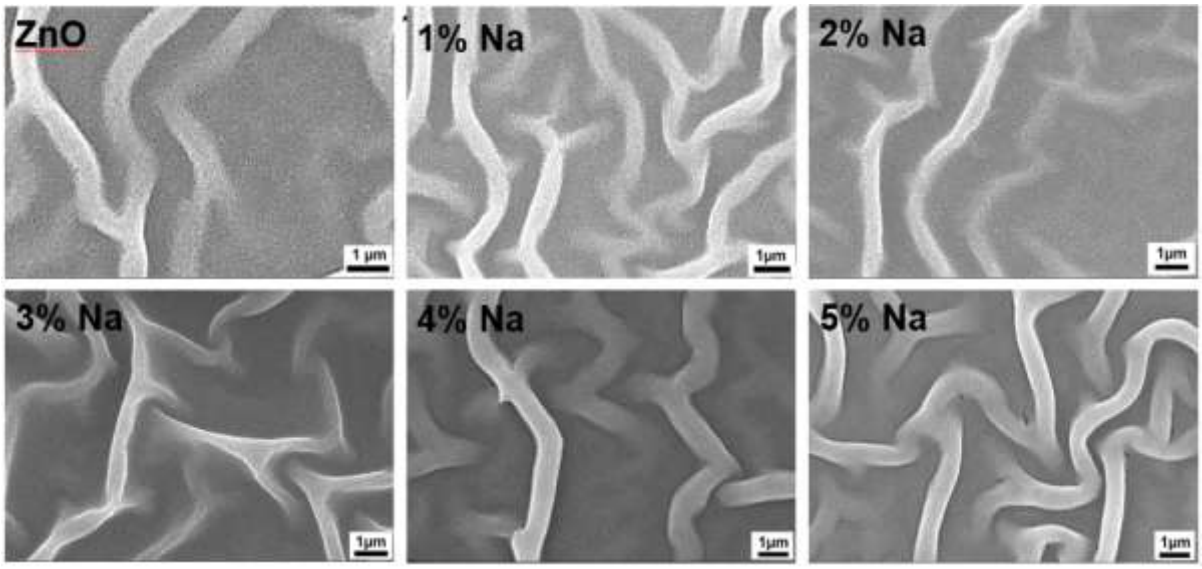

Figure 2. SEM micrographs of pure ZnO and Na-doped ZnO films.

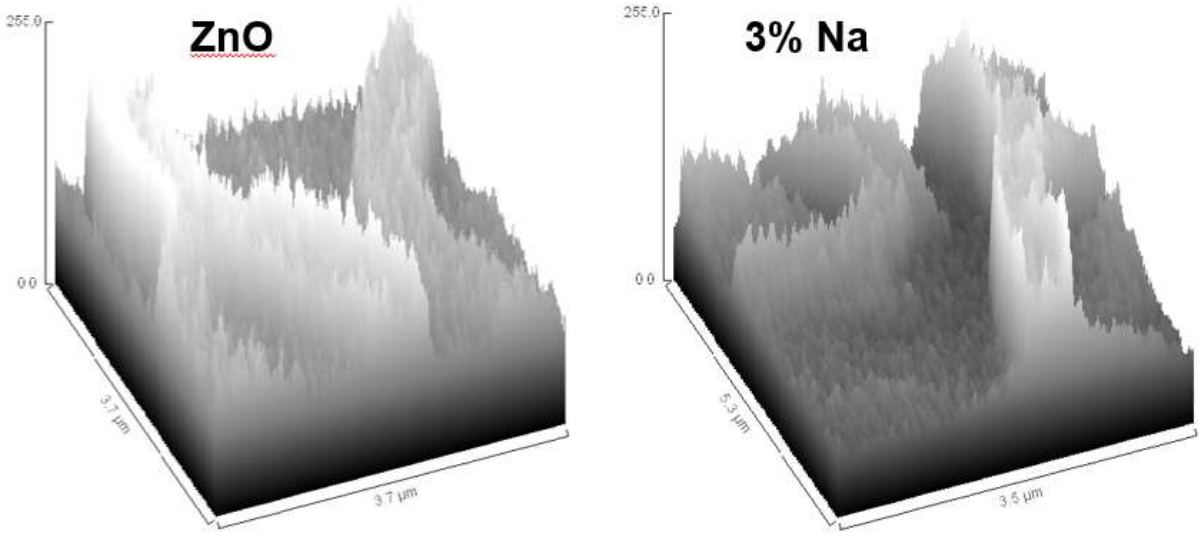

Figure 3. The roughness images of pure ZnO and 3% Ni-doped ZnO films.

3.3. Optical Property

The transmittance and absorbance spectra of NZO thin films with various doping concentrations were analyzed at the wavelength from 350 to 800 nm, as seen in Fig. 4a. The undoped ZnO has an average transmittance value of about 70%, while the doped samples have an average transmittance of about 78, 75, 60, 18, 25% for Na concentrations of 1, 2, 3, 4, 5 %, respectively. This result shows that Na significantly changed the transmittance of the film, making the film better absorbed at high Na concentrations. The transmittance of the film depends on many factors such as surface, particle size and film thickness. The change in transmittance of the NZO film may be attributed to the wrinkle structure of the film and the tight arrangement of the nanoparticles as observed in the SEM image as shown in Fig. 2. The wrinkle formation has a strong impact on optical phenomena such as transmittance and absorbance of materials. From the SEM image results and the transmittance in Fig. 4a, it is clear to see that the doping concentration play an important role in the formation progress and this factor can be controlled to obtain desired wrinkle height, which seems suitable to solar cells.

The optical bandgap energy can be determined by using the following equation:

$$(\alpha h\nu)^2 = k(h\nu - E_g) \tag{5}$$

where α is the absorption coefficient, h is Planck's constant, ν is the photon frequency and E_g is the optical bandgap energy [35]. So, the bandgap can be estimated by the extrapolation of the linear part of the $(\alpha h\nu)^2$ versus photon energy ($h\nu$) plot as shown in Fig. 4b.

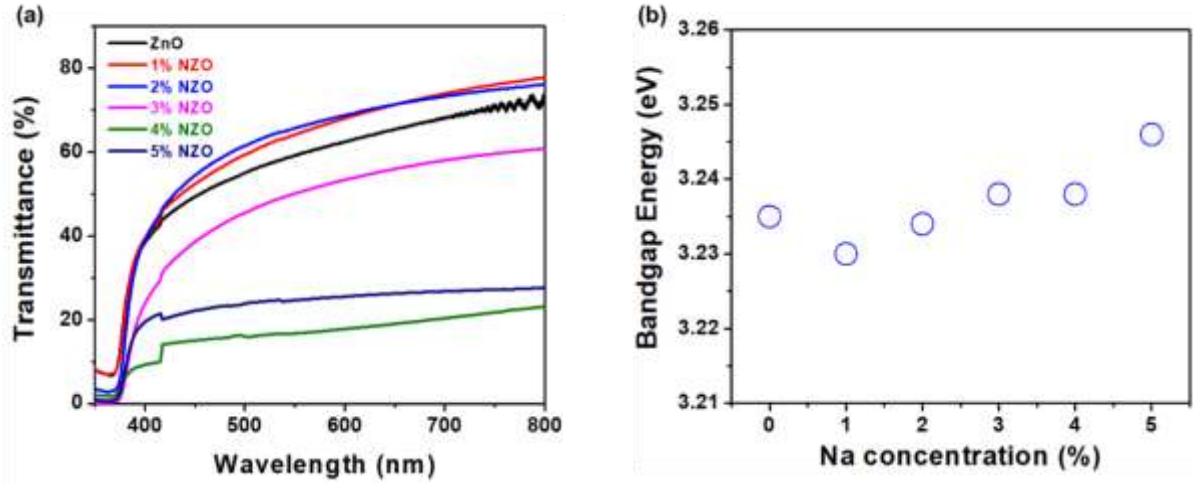

Figure 4. Transmittance (a) and the bandgap energy (b) of Na-doped ZnO thin films.

The optical bandgap energy, E_g, is 3.235 eV for pure ZnO, and it is 3.230, 3.234, 3.238, 3.238 and 3.246 eV for the films changed with 1, 2, 3, 4 and 5% doping, respectively. The E_g value of ZnO in our work agrees well with the value of 3.26 eV of Al-doped ZnO film fabricated by sol-gel method [36]. According to Chelouche et al., [37], the bandgap energy value decreased could be due to an increase in crystal size. Wu et al., [38] also reported that the bandgap reduction in Na-doped ZnO nanocrystal thin films deposited by sol-gel spin coating technique is due to the generation of a p-type conductive film. The increase in bandgap at concentrations above 2% Na doping can be attributed to a reduction in crystal size, which results in a quantum size effect. Furthermore, the increasing Na concentration increases the Na_i donor defects, which can result in impurity levels near the minimum conduction band (CBM), and these Na_i defects compensate for the acceptors Na_{Zn}, resulting in increased electron concentration [37].

3.4. Electrical Property

Table 2. The bandgap energy and the sheet resistance of NZO films with various Na doping concentrations

Na doping contents (%)	0	1	2	3	4	5
R_S (MΩ)	71.09	55.36	59.77	43.93	49.15	61.31
E_g (eV)	3.235	3.230	3.234	3.238	3.238	3.246

The sheet resistance (R_S) of the Na-doped ZnO thin films was determined at room temperature using a four-point probe measurement system, as shown in Table 2. The results show that the electrical properties of ZnO films are affected by the amount of Na doping. The Na ions improved the conductivity of the ZnO film. When 3% Na doping was added to the ZnO film, the resistance decreased significantly, with the lowest resistance being 43.93 MΩ/sq. The decrease in resistance can be attributed to an increase in particle density, which makes the surface denser and allows charges to move more easily, as seen in the SEM micrographs. When the Na content is low, the Na atom substitutes to V_{zn} and the Na_{Zn} acceptor forms in the ZnO structure, thus this leads to a decrease in the resistance of the NZO film [39]. According to Zheng et al., [40], increasing the concentration of Na doped degrades the crystal quality, leading to an increase in electrical resistance.

3.5. Absorption Figure of Merit (a-FOM) Analysis

Optical and electrical properties are two critical requirements for evaluating transparent ZnO films. Good absorption and high conductivity are required for photonic devices and solar cell applications. Because the Na-doped ZnO film has a rough surface and good absorbance at high concentrations, the data are calculated based on the extent of absorption. The *a-FOM* value is used as a criterion for the performance of transparent conducting film (TCO) film characteristics to evaluate the quality of NZO thin films, and it is calculated using the equation [41]:

$$a - FOM = (\rho d\alpha)^{-1} = \left(\rho d \frac{1}{L_\alpha}\right)^{-1} = \frac{L_\alpha}{\rho d} \quad (6)$$

where ρ is the resistivity, α is the absorption coefficient, d is the thickness of the film and L_α the absorption length that is expressed by the following equation [42, 43]:

$$\frac{1}{L_\alpha} = \frac{\int_{E_g}^{\infty} \alpha(E) u_{ph}(E) dE}{\int_{E_g}^{\infty} u_{ph}(E) dE} \quad (7)$$

where *α(E)* is the absorption coefficient as a function of the photon energy and u_{ph} is photon flux. The evaluation of the absorbance of the films against the solar spectrum via the absorption length aids in determining the films' absorption efficiency. The absorption length, which is inversely proportional to the absorption coefficient, describes how much light can enter a semiconductor material before it is completely absorbed. For increasing Na doping concentration, the value of NZO decreased, from 54.1 nm for undoped films to 54.3, 41.1, 25.1, 34.5 and 29.5 nm for 1 to 5% doped films. This also demonstrated that Na ions increased ZnO film light absorption. The transparent NZO film can stronger absorb light than the flat ZnO film thanks to its special ridge structure. Fig. 5 depicts the change in *a-FOM* with dopant Na concentration, with the *a-FOM* value increasing as the doping Na concentration increases. It reaches a largest value of 0.981 $\Omega^{-1}cm^{-1}$ for 1% Na-doped films and thereafter decreases.

The *a-FOM* for NZO films indicates that they can be used as transparent contacts in a variety of optoelectronic devices.

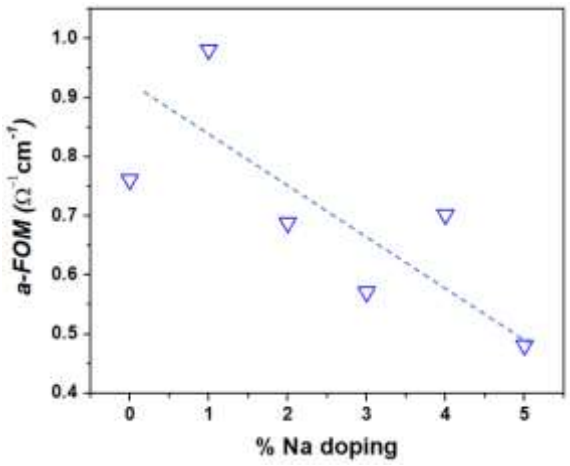

Figure 5. Absorption figure of merit for un-doped and doped ZnO films with various Na doping levels.

4. Conclusion

In this work, NZO thin films were synthesized by sol-gel and spin-coating techniques. According to the XRD results, the NZO thin film exhibited a polycrystalline wurtzite hexagonal structure with a preferential orientation of (110). The crystal size of the film decreased with the increasing concentration of Na doping. The surface of the NZO films retained the wrinkled structure of the pure ZnO film, indicating that Na did not change the surface structure of ZnO. The wrinkle structure improved the film's ability to absorb light. The transmittance of the films changed markedly when doping with Na, specifically, the transmittance of un-doped film was 78%, and decreased to 25% at 5% Na dopant. In addition, the Na/Zn ratio affected the optical band energy, i.e., it ranged between 3.235 and 3.246 eV, while the resistivity was lowest at 3% Na doping. Hence, the *a-FOM* value tends to decrease with increasing Na concentration.

Acknowledgement

This work is fully supported by the project with the code number of VJU.JICA.21.03, from Vietnam Japan University, under Research Grant Program of Japan International Cooperation Agency.

References

[1] Ü. Özgür, Y. I. Alivov, C. Liu, A. Teke, M. A. Reshchikov, S. Doğan, V. Avrutin, S. J. Cho, H. Morkoç, A Comprehensive Review of ZnO Materials and Devices, J. Appl. Phys., Vol. 98, 2005, pp. 041301.

[2] Q. Li, K. Cheng, W. Weng, P. Du, G. Han, Synthesis, Characterization and Electrochemical Behaviour of Sb-Doped ZnO Microsphere Film, Thin Solid Films, Vol. 544, 2013, pp. 466-471.

[3] M. D. McCluskey, S. J. Jokela, Defects in ZnO, J. Appl. Phys., Vol. 106, 2009, pp. 071101.

[4] J. C. Fan, K. M. Sreekanth, Z. Xie, S. L. Chang, K. V. Rao, P-type ZnO Materials: Theory, Growth, Properties and Devices, Prog. Mater. Sci., Vol. 58, 2013, pp. 874-985.

[5] Z. N. Ng, K. Y. Chan, S. Muslimin, D. Knipp, P-type Characteristic of Nitrogen-doped ZnO Films, J. Electron. Mater., Vol. 47, 2018, pp. 5607-5613.

[6] K. K. Kim, H. S. Kim, D. K. Hwang, J. H. Lim, S. J. Park, Realization of p-type ZnO Thin Films Via Phosphorus Doping and Thermal Activation of the Dopant, Appl. Phys. Lett., Vol. 83, 2003, pp. 63-65.

[7] P. Biswas, P. Nath, D. Sanyal, P. Banerji, An Alternative Approach to Investigate the Origin of P-type Conductivity in Arsenic Doped ZnO, Current Applied Physics, Vol. 15, 2015, pp. 1256-1261.

[8] S. V. Mohite, K. Y. Rajpure, Synthesis and Characterization of Sb Doped ZnO Thin Films for Photodetector Application, Opt. Mater., Vol. 36, 2014, pp. 833-838.

[9] L. M. Mahajan, C. K. Kasar, D. S. Patil, Investigation of Optical and Electrical Properties of Lithium Doped ZnO Nano Films, Mater. Res. Express, Vol. 6, 2019, pp. 045053.

[10] S. Lin, J. Lu, Z. Ye, H. He, X. Gu, L. Chen, J. Huang, B. J. S. S. C. Zhao, P-type Behaviour in Na-doped ZnO Films and ZnO Homojunction Light-Emitting Diodes, Vol. 148, 2008, pp. 25-28.

[11] S. Guan, L. Wang, Y. Tamamoto, M. Kato, Y. Lu, X. Zhao, Fabrication and Characterization of Potassium-Doped ZnO Thin Films, J. Mater. Sci.: Mater. Electron., Vol. 32, 2021, pp. 669-675.

[12] E. C. Lee, K. J. Chang, Possible P-type Doping with Group-I Elements in ZnO, Phys. Rev. B, Vol. 70, 2004, pp. 115210.

[13] C. H. Park, S. B. Zhang, S. H. Wei, Origin of P-type Doping Difficulty in ZnO: The Impurity Perspective, Phys. Rev. B, Vol. 66, 2002, pp. 073202.

[14] S. S. Lin, J. G. Lu, Z. Z. Ye, H. P. He, X. Q. Gu, L. X. Chen, J. Y. Huang, B. H. Zhao, P-type Behavior in Na-Doped ZnO Films and ZnO Homojunction Light-emitting Diodes, Solid State Commun, Vol. 148, 2008, pp. 25-28.

[15] P. Ding, X. H. Pan, Z. Z. Ye, J. Y. Huang, H. H. Zhang, W. Chen, C. Y. Zhu, Realization of P-type Non-polar A-Plane ZnO Films Via Doping of Na Acceptor, Solid State Commun., Vol. 156, 2013, pp. 8-11.

[16] L. W. Wang, F. Wu, D. X. Tian, W.J. Li, L. Fang, C. Y. Kong, M. Zhou, Effects of Na Content on Structural and Optical Properties of Na-doped ZnO Thin Films Prepared by Sol–gel Method, J. Alloys Compd., Vol. 623, 2015, pp. 367-373.

[17] J. G. Cuadra, S. Porcar, D. Fraga, T. S. Lyubenova, J. B. Carda, Enhanced Electrical Properties of Alkali-doped Zno Thin Films with Chemical Process, Solar, Vol. 1, 2021, pp. 30-40.

[18] S. K. Kim, S. A. Kim, C. H. Lee, H. J. Lee, S. Y. Jeong, C. R. Cho, The Structural and Optical Behaviors of K-Doped ZnO⁄Al_2O_3 (0001) Films, Appl. Phys. Lett., Vol. 85, 2004, pp. 419-421.

[19] L. Xu, X. Li, J. Yuan, Effect of K-doping on Structural and Optical Properties of ZnO Thin Films, Superlattices Microstruct., Vol. 44, 2008, pp. 276-281.

[20] H. B. Liu, X. H. Pan, J. Y. Huang, H. P. He, Z. Z. Ye, Preparation of Na Delta-doped P-type ZnO Thin Films by Pulsed Laser Deposition Using NaF and ZnO Ceramic Targets, Thin Solid Films, Vol. 540, 2013, pp. 53-57.

[21] H. Shen, X. Zhao, L. Duan, R. Liu, H. Li, B. Wang, Effect of Na_{Zn}/Na_i Ratio on Structural, Optical, and Electrical Properties of Na-doped ZnO Thin Films, J. Appl. Phys., Vol. 121, 2017, pp. 155303.

[22] R. Maity, S. Das, M. K. Mitra, K. K. Chattopadhyay, Synthesis and Characterization of ZnO Nano/Microfibers Thin Films by Catalyst Free Solution Route, Phys. E, Vol. 25, 2005, pp. 605-612.

[23] S. Kumar, R. Thangavel, Structural and Optical Properties of Na Doped ZnO Nanocrystalline Thin Films Synthesized Using Sol–gel Spin Coating Technique, J. Sol-Gel Sci. Technol., Vol. 67, 2013, pp. 50-55.

[24] J. Lü, K. Huang, J. Zhu, X. Chen, X. Song, Z. Sun, Preparation and Characterization of Na-doped ZnO Thin Films by Sol–gel Method, Phys. B, Vol. 405, 2010, pp. 3167-3171.

[25] S. Ilican, Y. Caglar, M. Caglar, F. Yakuphanoglu, Electrical Conductivity, Optical and Structural Properties of Indium-doped ZnO Nanofiber Thin Film Deposited by Spray Pyrolysis Method, Phys. E, Vol. 35, 2006, pp. 131-138.

[26] X. S. Wang, Z. C. Wu, J. F. Webb, Z. G. Liu, Ferroelectric and Dielectric Properties of Li-doped ZnO Thin Films Prepared by Pulsed Laser Deposition, Appl. Phys. A, Vol. 77, 2003, pp. 561-565.

[27] K. Navin, R. Kurchania, Structural, Morphological and Optical Studies of Ripple-Structured ZnO Thin Films, Appl. Phys. A, Vol. 121, 2015, pp. 1155-1161.

[28] H. T. Kim, S. Y. Lee, C. Park, Controls of Surface Morphology on Sol-Gel Derived ZnO Films Under Isothermal Treatment Conditions, Vacuum, Vol. 143, 2017, pp. 312-315.

[29] S. J. Kwon, J. H. Park, J. G. Park, Wrinkling of a Sol-gel-derived Thin Film, Phys. Rev. E, Vol. 71, 2005, pp. 011604.

[30] M. S. Kim, K. G. Yim, D. Y. Lee, J. S. Kim, J. S. Kim, J. S. Son, J. Y. Leem, Effects of Cooling Rate and Post-Heat Treatment on Properties of ZnO Thin Films Deposited by Sol–gel Method, Appl. Surf. Sci., Vol. 257, 2011, pp. 9019-9023.

[31] D. C. Lim, W. H. Shim, K. D. Kim, H. O. Seo, J. H. Lim, Y. Jeong, Y. D. Kim, K. H. Lee, Spontaneous Formation of Nanoripples on the Surface of ZnO Thin Films As Hole-Blocking Layer of Inverted Organic Solar Cells, Sol. Energy Mater. Sol. Cells, Vol. 95, 2011, pp. 3036-3040.

[32] G. W. Scherer, Sintering of Sol-gel Films, J. Sol-Gel Sci. Technol., Vol. 8, 1997, pp. 353-363.

[33] N. Sekine, C. H. Chou, W. L. Kwan, Y. Yang, ZnO Nano-Ridge Structure and Its Application in Inverted Polymer Solar Cell, Org. Electron., Vol. 10, 2009, pp. 1473-1477.

[34] J. W. Choi, J. W. Jin, D. Tondelier, Y. Bonnassieux, B. Geffroy, Low Temperature Solution-processable 3D-Patterned Charge Recombination Layer for Organic Tandem Solar Cells, Materials, Vol. 12, 2019, pp. 162.

[35] X. L. Zhang, K. S. Hui, K. N. Hui, High Photo-responsivity ZnO UV Detectors Fabricated by RF Reactive Sputtering, Mater. Res. Bull., Vol. 48, 2013, pp. 305-309.

[36] B. N. Q. Trinh, T. D. Chien, N. Q. Hoa, D. H. Minh, Solution-processable Zinc Oxide Based Thin Films with Different Aluminum Doping Concentrations, J. Sci.: Adv. Mater. Devices, Vol. 5, 2020, pp. 497-501.

[37] A. Chelouche, T. Touam, F. Boudjouan, D. Djouadi, R. Mahiou, A. Bouloufa, G. Chadeyron, Z. Hadjoub, Na Doping Effects on the Structural, Conduction Type and Optical Properties of Sol–gel ZnO Thin Films, J. Mater. Sci.: Mater. Electron., Vol. 28, 2017, pp. 1546-1554.

[38] S. H. Wu, S. Kumar, R. Thangavel, S. U. Jen, W. C. Cheng, Y. C. Chang, Erratum to: Structural and Optical Properties of Na Doped ZnO Nanocrystalline Thin Films Synthesized Using Sol–gel Spin Coating Technique, J. Sol-Gel Sci. Technol., Vol. 71, 2014, pp. 192.

[39] S. S. Lin, Z. Z. Ye, J. G. Lu, H. P. He, L. X. Chen, X. Q. Gu, J. Y. Huang, L. P. Zhu, B. H. Zhao, Na Doping Concentration Tuned Conductivity of ZnO Films Via Pulsed Laser Deposition and Electroluminescence from ZnO homojunction on Silicon Substrate, J. Phys. D: Appl. Phys., Vol. 41, 2008, pp. 155114.

[40] Z. Zheng, Y. F. Lu, Z. Z. Ye, H. P. He, B. H. Zhao, Carrier Type- and Concentration-Dependent Absorption and Photoluminescence of ZnO Films Doped with Different Na Contents, Mater. Sci. Semicond. Process, Vol. 16, 2013, pp. 647-651.

[41] H. Q. Nguyen, D. V.Nguyen, A. Fujiwara, B. N. Q. Trinh, Solution-processed CuO Thin Films with Various Cu^{2+} Ion Concentrations, Thin Solid Films, Vol. 660, 2018, pp. 819-823.

[42] J. J. Loferski, Thin Films and Solar Energy Applications, Surf. Sci., Vol. 86, 1979, pp. 424-443.

[43] F. Alharbi, J. D. Bass, A. Salhi, A. Alyamani, H. C. Kim, R. D. Miller, Abundant Non-Toxic Materials for Thin Film Solar Cells: Alternative to Conventional Materials, Renewable Energy, Vol. 36, 2011, pp. 2753-2758.